Tunable Protein and Bacterial Cell Adsorption on Colloidally-Templated Superhydrophobic Polythiophene Films

Journal:	*Chemistry of Materials*
Manuscript ID:	cm-2011-007044.R1
Manuscript Type:	Article
Date Submitted by the Author:	13-May-2011
Complete List of Authors:	Pernites, Roderick; University of Houston, Chemistry Santos, Catherine; University of Houston, Civil and Environmental Engineering Maldonado, Miguel; University of Houston, Chemistry Ponnapati, Ramakrishna; University of Houston Rodrigues, Debora; University of Houston, Civil and Environmental Engineering Advincula, Rigoberto; University of Houston, Chemistry

SCHOLARONE™
Manuscripts

Tunable Protein and Bacterial Cell Adsorption on Colloidally-Templated Superhydrophobic Polythiophene Films

Roderick B. Pernites,[1] Catherine M. Santos,[3] Miguel Maldonado,[2] Ramakrishna R. Ponnapati,[2] Debora F. Rodrigues,[3] and Rigoberto C. Advincula[1,2]*

[1]Department of Chemistry and [2]Department of Chemical and Biomolecular Engineering,

[3]Department of Civil and Environmental Engineering

University of Houston, Houston, Texas, 77204-5003

RECEIVED DATE (to be automatically inserted after your manuscript is accepted if required according to the journal that you are submitting your paper to)

*Corresponding author. E-mail: radvincula@uh.edu; Phone: +1 713 743 1755

ABSTRACT

A facile approach for enabling *or* inhibiting the adsorption of protein and adhesion of bacterial cells on a potential-induced reversibly wettable polythiophene film is described. The superhydrophobic polymeric surface was first prepared by a two-step process that combines the layering of polystyrene (PS) latex particles *via* a Langmuir-Blodgett (LB)-*like* technique followed by Cyclic Voltammetric (CV) - electrodeposition of polythiophene from a terthiophene ester monomer. The polythiophene conducting polymer coating enabled control of the wettability of the surface by simply changing its redox property *via* potential switching. The influence of morphology on this switching behavior is also described. The wettability in return controls the adsorption of protein and adhesion of bacterial cells. For instance, the undoped polythiophene film, which is superhydrophobic, inhibits the adhesion of fibrinogen proteins and *Escherichia coli* (*E. coli*) cells. On the other hand, the doped film, which is hydrophilic, leads to increased attachment of both protein and bacteria. Unlike most synthetic anti-wetting surfaces, the as-prepared superhydrophobic coating is non-fluorinated. It maintains its superhydrophobic property at a wide range of pH (pH 1-13) and temperature (below -10 ^{o}C and between 4 ^{o}C and 80 ^{o}C). Moreover, the surface demonstrated self-cleaning properties at a sliding angle as low as $3^{o} \pm 1$. The proposed methodology and material should find application in the preparation of smart or tunable biomaterial surfaces that can be either resistant or susceptible to proteins and bacterial cell adhesion by a simple potential switching.

Table of Contents

Roderick B. Pernites, Catherine M. Santos, Miguel Maldonado, Ramakrishna R. Ponnapati, Debora F. Rodrigues, and Rigoberto C. Advincula*

A superhydrophobic polymeric surface is fabricated by a two-step colloidal-template electropolymerization approach using a *non-fluorinated* conducting polymer of polythiophene. By changing the redox property of the conducting polymer, the surface is able to promote or inhibit the adsorption of proteins or bacterial cells.
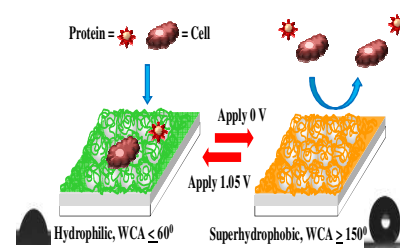
1. INTRODUCTION

The phenomenon of superhydrophobicity and the preparation of synthetic superhydrophobic surfaces have recently attracted much attention due to its potential industrial and biomedical applications.[1] The design of artificial anti-wetting surfaces is nature inspired. For instance, the natural superhydrophobic surfaces, which are found in many plant leaves like the Lotus leaf,[2] the Lady's Mantle,[3] and in many insects[4] like the water strider, butterfly, and the cicada, contain hierarchical roughness that has been mimicked in hydrophobic materials. Ma and Hill[5] summarized the different materials and the common strategies utilized for structuring the surface to template the natural design. Most of these methods include tedious lithographic steps and require intricate instrumental set-up, which can limit their realistic application for surface coatings. Although not widely reported, electrochemical polymerization or electrodeposition of polymers can be an alternative for making superhydrophobic surfaces.[6] However, most of the reports on electrodeposition of π-conjugated polymers for anti-wetting purposes use fluorinated substituents, which are not only more expensive but bio-accumulates in the environment.[7] Therefore, these concerns necessitate the search for non-fluorinated π-conjugated polymer alternatives. Among the π-conjugated polymers, poly(thiophenes) and its derivatives are well-known and are relatively stable for practical applications.[8]

Despite the numerous and successful bio-mimetic efforts to achieve superhydrophobic surfaces,[5,6] there are only few studies on investigating their potential for biomaterial applications. Genzer and Efimenko[9] reported recent developments on superhydrophobic coatings and noted the limited work on their applications to prevent biofouling on surfaces or on biomedical devices.[10] The resistance as well as the adsorption of protein or bacteria to material surfaces can have diverse medical, industrial, and environmental applications and implications. For instance, the adsorption of protein to surfaces is important to the development of biosensors and immunoassays.[11] Materials like di-block copolymers that are physically or chemically adsorbed to the surface have been used for controlling the adhesion of proteins.[12] In the case of bacterial adhesion to surfaces and biofilm formation, these phenomena can help

in the degradation of organic matter in wastewater treatment,[13] bioremediation,[14] selective extraction of metals from ores,[15] and on basic studies for *in vitro* growth of bacterial cells. On the other hand, the adhesion of proteins or bacteria can cause impairment of the surface functionality of biomedical devices[16] such as of catheters,[17] implants,[18] and artificial organs.[17a, 19] Furthermore, adhesion of bacteria on the water distribution system can clog pipes and generate corrosion.[20, 21] Therefore, numerous efforts have been directed to modify the surface with a material that would resist bacterial adsorption and colonization, as well as adsorption of proteins.[22] One possible approach to prevent biofouling is to make the surface superhydrophobic, i.e. by controlling the surface energy and surface topography of the substrate.[23] Marmur[24] claimed that biofouling hindrance can be obtained by minimizing the contact between water and surface using a superhydrophobic coating, since foulers are generally biological materials suspended in water with high affinity for hydrophilic surfaces. Moreover, Rubner et al.[25] underscored that superhydrophobic surfaces can actually provide resistance or reduced capacity of bacteria to achieve stage I and/or stage II in bacterial adhesion.

Since material surfaces that control adhesion of protein and bacteria cells are medically, industrially, and environmentally relevant, it will be interesting to create a tunable surface that can also facilitate self-cleaning. So far, most reports have focused only on making a surface that is either resistant or susceptible to protein or bacteria adhesion but not tunable. In the present work, we developed a facile approach to enable controlled adhesion of proteins and bacterial cells to surfaces. These surfaces are coated with highly stable and albeit nonfluorinated electrodeposited superhydrophobic polythiophene, utilizing a colloidal template-assisted electropolymerization technique. This study also provides an insight on controlling the wettability of the surface by a simple potential switching of the redox property of the conducting polymer surface. Finally, the effect of changing the redox property of the polymeric surface was explored with the adsorption or inhibition of fibrinogen and *E. coli* attachment to the surfaces. To the best of our knowledge, this is one of the first reports on controlled attachment and prevention of protein and bacteria adhesion utilizing a potential-induced and reversibly-wettable

polythiophene film. The advantage of using a conducting polymer coating is the ability to control the wettability and electro-optical properties of the polymeric surface simultaneously by simply changing its redox property. i.e. enabling self-cleaning function by an ex-situ change in potential. Recently, we have demonstrated the effect of altering the redox property of polythiophene film that is electrodeposited on flat surfaces to facilitate the effective release of drug molecules from an ultrathin film of molecularly imprinted polythiophene surface.[26]

2. RESULTS AND DISCUSSION
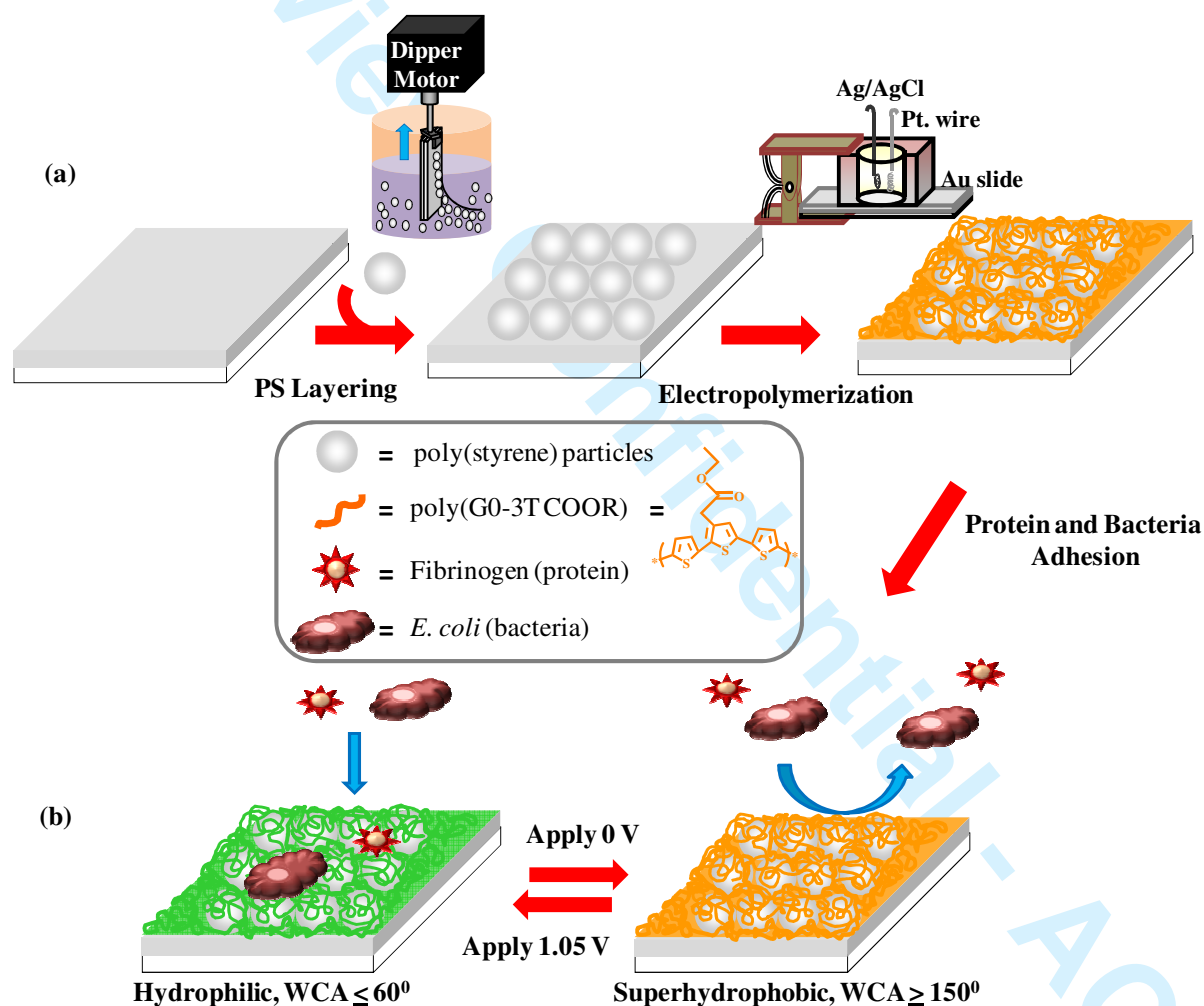
2.1 Film Preparation and Characterization

Figure 1. (a) Fabrication scheme of the superhydrophobic polymeric surface by PS layering and CV (cyclic voltammetry)-electropolymerization. (b) Protein (fibrinogen) and bacterial (*E. coli*) adhesion onto the undoped (orange-colored film) and doped (green-colored film) colloidally-templated polythiophene (poly(G0-3T COOR)/PS) surfaces.

The anti-wetting surface was fabricated using a two-step approach. Figure 1 depicts the schematic representation of the film fabrication starting with the colloidal template (PS particle) layering onto a planar conducting substrate by a Langmuir-Blodgett (LB)-*like* technique.[27] This method was used because it allows two dimensional (2D) monolayer and closely-packed ordering of particles on flat surfaces, which is dependent on the vertical lifting speed of the substrate and colloidal particle and surfactant concentrations[27] Figure 2 displays the atomic force microscopy (AFM) topography 2D (Fig. 2a) and 3D (Fig. 2b) images of the single layer 500 nm sized PS particles adsorbed on Au substrate and the scanning electron microscopy (SEM) images after polythiophene electrodeposition (Fig 2c and 2d) of the doped and undoped films respectively. The AFM images reveal a highly ordered monolayer assembly of colloidal particles in hexagonal packing or honeycomb arrangement as clearly seen in the high magnification image (inset of Figure 2a). Similar surface patterns were also observed for other sizes of PS when the deposition was done on an Indium Tin Oxide (ITO) substrate (see Supporting information, Figure S1). Attenuated total reflection infrared (ATR IR) spectrum of the PS layer on Au is presented in Figure S1d, which shows the signature peaks of PS, confirming its presence on the surface.
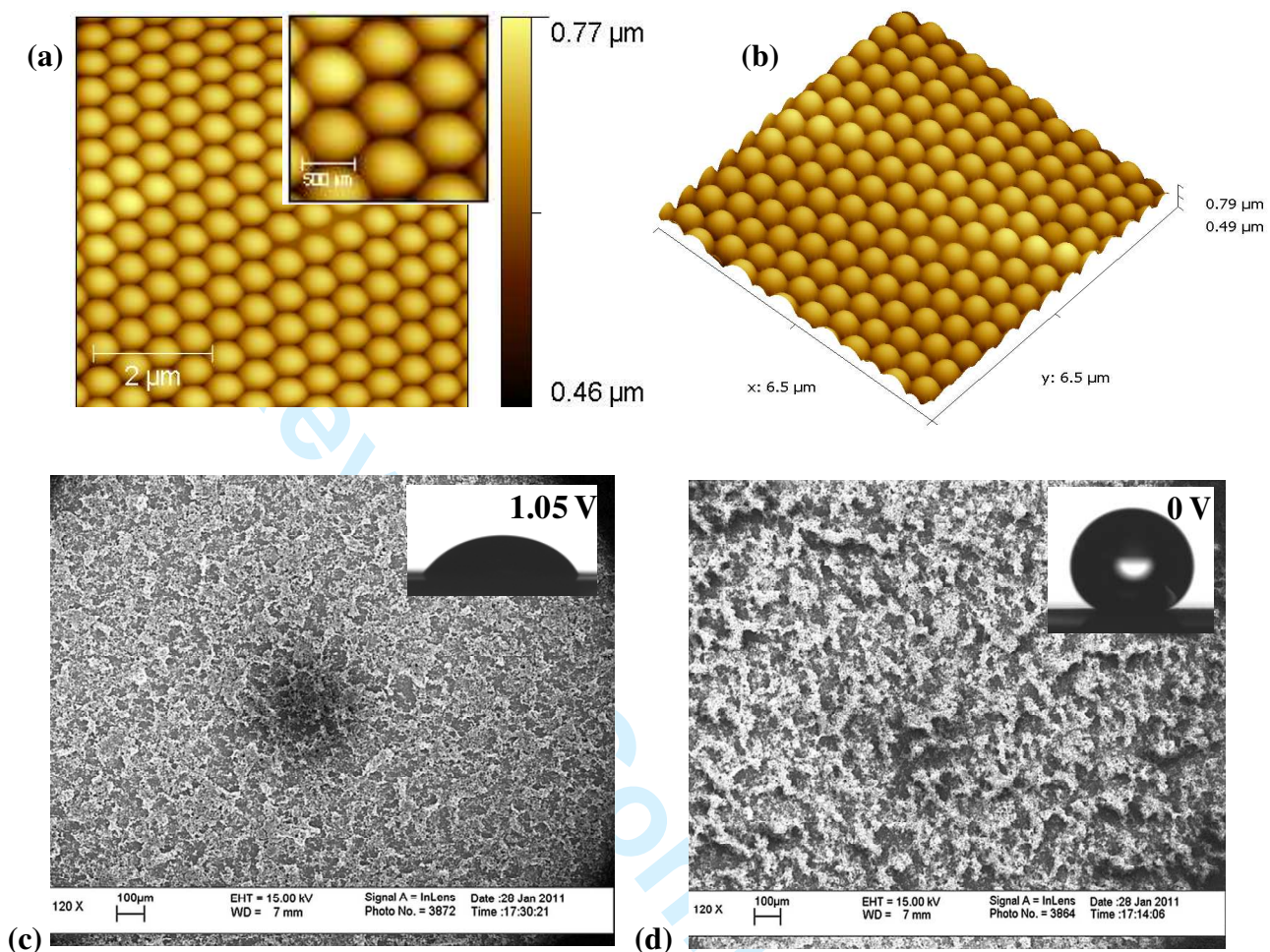
Figure 2. AFM topography (a) 2D and (b) 3D images of the 500 nm size PS coated-Au substrate with high magnification image on inset of (a). Note: AFM scan area is 6.5 µm x 6.5 µm. SEM wide scan of the (c) doped and (d) undoped or dedoped colloidally-templated and electrodeposited polythiophene surface (poly(G0-3T COOR)/PS Au)). Inset shows the wetting behavior (contact angle) and the respective applied voltage.

Electrodeposition of the polythiophene layer on the PS-coated conducting substrate was performed by CV technique. This method allows direct grafting of the conducting polymer onto the electrode surface, control of polymer film thickness, surface growth, and morphology by varying various set-up parameters such as scan rate, CV cycles, and potential window.[28] The morphology by SEM imaging is shown in Figure 2 (c) and (d) for the doped and dedoped films, respectively. Further discussion on morphology vis-à-vis wetting properties is elaborated on the succeeding sections. Figure 3a presents the

8

typical CV diagram of the anodic electropolymerization of the (ethyl 2-(2,5-di(thiophen-2-yl)thiophen-3-yl)acetate (G0-3T COOR) monomer.[29] The advantage of using the terthiophene monomer for electropolymerization is the lower oxidation potential compared to its mono or bithiophene counterparts.[30] This process is evidenced by the increasing current in the oxidation (between 0.8 V to 1.1 V) and reduction (between 0.6 V to 1.0 V) peaks until the 15th cycle (Fig. 3a), which is attributed to the linking of the terthiophene units and electrodeposition of the material onto the electrode substrate.[29] The current increase in the anodic scan that occurs from the 2nd cycle with an onset potential of ~0.6 V is attributed to the oxidation of the more conjugated species.[29] The deposition of the polymer film onto the electrode substrate was confirmed by the appearance of the same redox couple in the monomer-free post-polymerization scan (inset of Fig. 3a). During the electropolymerization, a very slow scan rate (5 mV/s) was applied to enable deposition of a thicker polymer film on top of the colloidally-templated electrode substrate. A film thickness between 2.5 to 6.5 µm was determined from profilometry measurements.

The electrodeposition of the conducting polymer onto the PS-coated substrate was verified by X-ray photoelectron spectroscopy (XPS). The survey scan (Fig. 3b) exhibits the expected elemental composition for poly(G0-3T COOR) such as carbon (C), oxygen (O), and sulfur (S) atoms.[26a] The S 2p peak (inset of Fig. 3b) in the high resolution scan at the range of 162 – 165 eV is a signature peak for polythiophene,[26a] which is due to the sulfur atom of the thiophene ring.
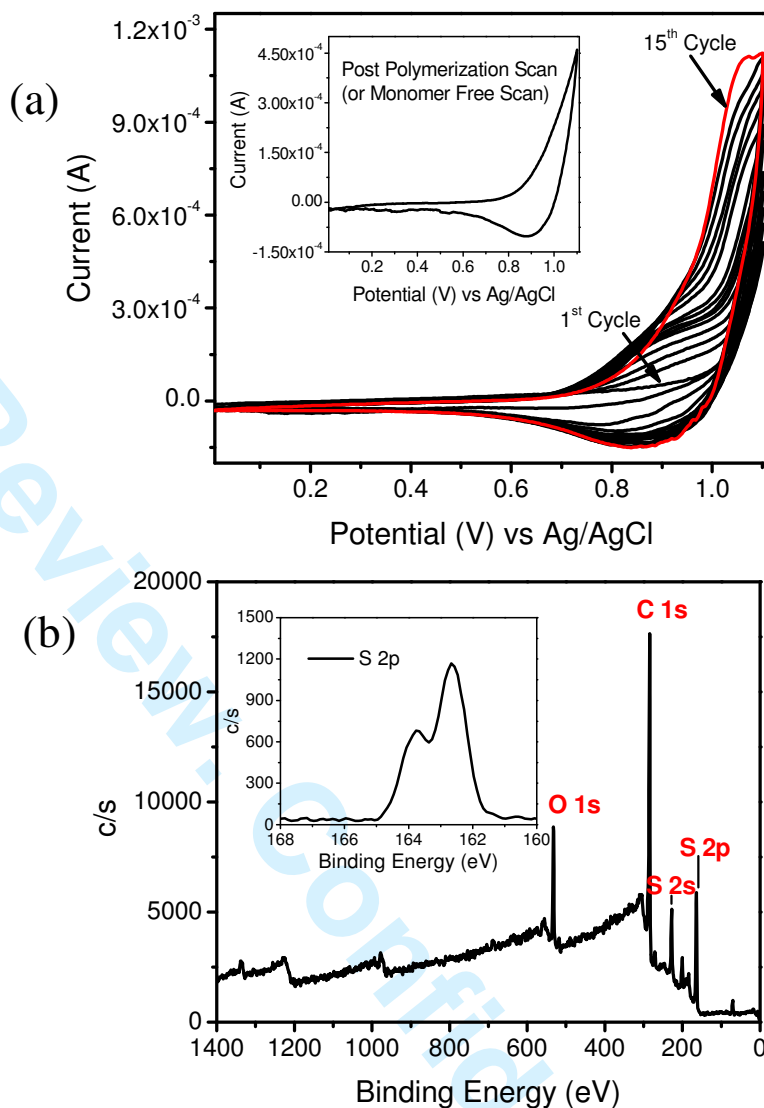
Figure 3. (a) CV electrodeposition of the conducting polymer (poly(G0-3T COOR)) with inset of the monomer-free post-polymerization scan in 0.1 M TBAH/ACN. (b) XPS wide scan of the electropolymerized film with inset of the S 2p high resolution scan.

2.2 Testing for Superhydrophobicity and Self-Cleaning Effect

The wettability of the poly(G0-3T COOR)/PS surface was evaluated. The surface exhibited a static water contact angle (WCA) value of $154^{\circ} \pm 1$ (Fig. S3a) at ambient conditions, which is attributed to the synergestic effect of the combined heirarchical roughness, which is seen in the scanning electron microscopy (SEM) images, and the presence of the hydrophobic conducting polymer coating on the surface. To underscore the importance of the PS template underlayer array, the poly(G0-3T COOR) film was electrodeposited using the same CV condition on a flat surface, and the contact angle was also

measured, which showed a value of only $103^{\circ} \pm 1$. This result shows the importance of the 500 nm sized PS template array underlayer to give a superhydrophobic effect on the surface. The PS monolayer array actually provides an initial sub-micron scale roughness to enhance the hydrophobicity of the surface.

The structuring of the surface was determined by SEM analysis. The SEM imaging (Fig. S3) displayed an irregularly rough surface of the as-prepared superhydrophobic film. This complex surface morphology was expected because the electropolymerization was done in a non-planar 2D substrate with a very slow scan rate. Based from the SEM low magnification image (Fig. S3b), the irregular roughness on the surface shows hierarchy or stepping order, which can serve as a multiple barrier for resisting the adhesion of water to the surface. For instance, the topmost layer comprises mainly of highly porous foam-like features that are above the micron scale bumps with size much greater than the PS particle. In some regions, highly dense foam-like structures of the conducting polymer are also seen on the surface (Fig. S3c). The underlayer (at low region below the foam-like features) clearly shows the continuous honeycomb assembly of the PS particle that is smeared with nanometer-sized asperities due to the conducting polymer (Fig. S3d). This result proves that the superhydrophobicity is not necessarily dependent on the regularity of the surface roughness like the surface of the Lotus leaf[2] and many other synthetic analogues prepared by sophisticated lithographic techniques, but by the presence of hierarchical features contributing to the non-wetting phenomenon[5] which is essentially a Cassie-Baxter Model.[33]

These films showed superior temperature and pH stability. The superhydrophobicity of the poly(G0-3T COOR)/PS surface was tested at various water droplet temperatures ranging from 4 $^{\circ}$C to 80 $^{\circ}$C. It was observed that the surface remained superhydrophobic (WCA $\geq 150^{\circ}$) at all measured temperatures (Fig. 4a). Furthermore, the superhydrophobicity was maintained even when the surface was incubated at below freezing condition (-10 $^{\circ}$C) for 1 and 4 days giving WCA values of $152^{\circ} \pm 3$ and $153^{\circ} \pm 2$,

respectively. The surface also maintained its superhydrophobicity at a wide pH range (pH 1-13) (Fig. 4b). The high water repellency of the same surface that is preserved at very low and very high pH values and at low and high temperatures of water is unusual and is not easily achieved in many synthetic superhydrophobic surfaces.

The static contact angle analysis was validated by dynamic measurement that displayed a high advancing (θ_{adv}) and receding (θ_{rec}) water contact angle values of $154^o \pm 1$ and $151^o \pm 1$, respectively. The difference in the two values is the contact angle hysteresis,[31] which is also used to gauge on whether the superhydrophobic surface will demonstrate the sliding of the water droplet.[1b, 32] Since the superhydrophobic surface has a very low hysteresis of $< 5^o$, it will most likely exhibit the rolling of the water droplet akin to the Lotus leaf. [1a, 32a]

The self-cleaning property of the as-prepared superhydrophobic polythiophene surface was confirmed, which allowed the rolling of the water droplet at the sliding angle of $3^o \pm 1$. Figure 4c displays images of the water droplet, hanging at the tip of the needle and at the same time touching the polymeric surface on the other side, displaying its ability to move freely across the superhydrophobic surface. These images vividly reveal that the surface is highly repellent to water. Because the water droplet was able to roll freely on the surface at a very low sliding angle, the superhydrophobic surface is characterized by the Cassie-Baxter model, [32a, 33] which explains that the water droplet is sitting and not pinned above the composite surface of the solid protuberances and air (described as heterogeneous wetting regime[34]). With the high porosity of the actual surface, as determined from the SEM analysis, the superhydrophobic surface is believed to entrap more air, particularly onto the micron scale asperities (Fig. S3b) and foam-like structures (Fig. S3c), and thus creating a liquid-gas layer upon contact with water, which is likely the reason for the sliding of the water droplet across the anti-wetting surface. Figure 4d (top left) shows the image of the pristine superhydrophobic coating electrodeposited on ITO, while Figure 4d (bottom left) displays the image of the same but dusted surface after rolling the water

droplet. Clearly, it is shown that the dust particles are completely removed and picked up by the water droplet that rolled off the surface, and hence the superhydrophobic surface has been proven to be self-cleaning.
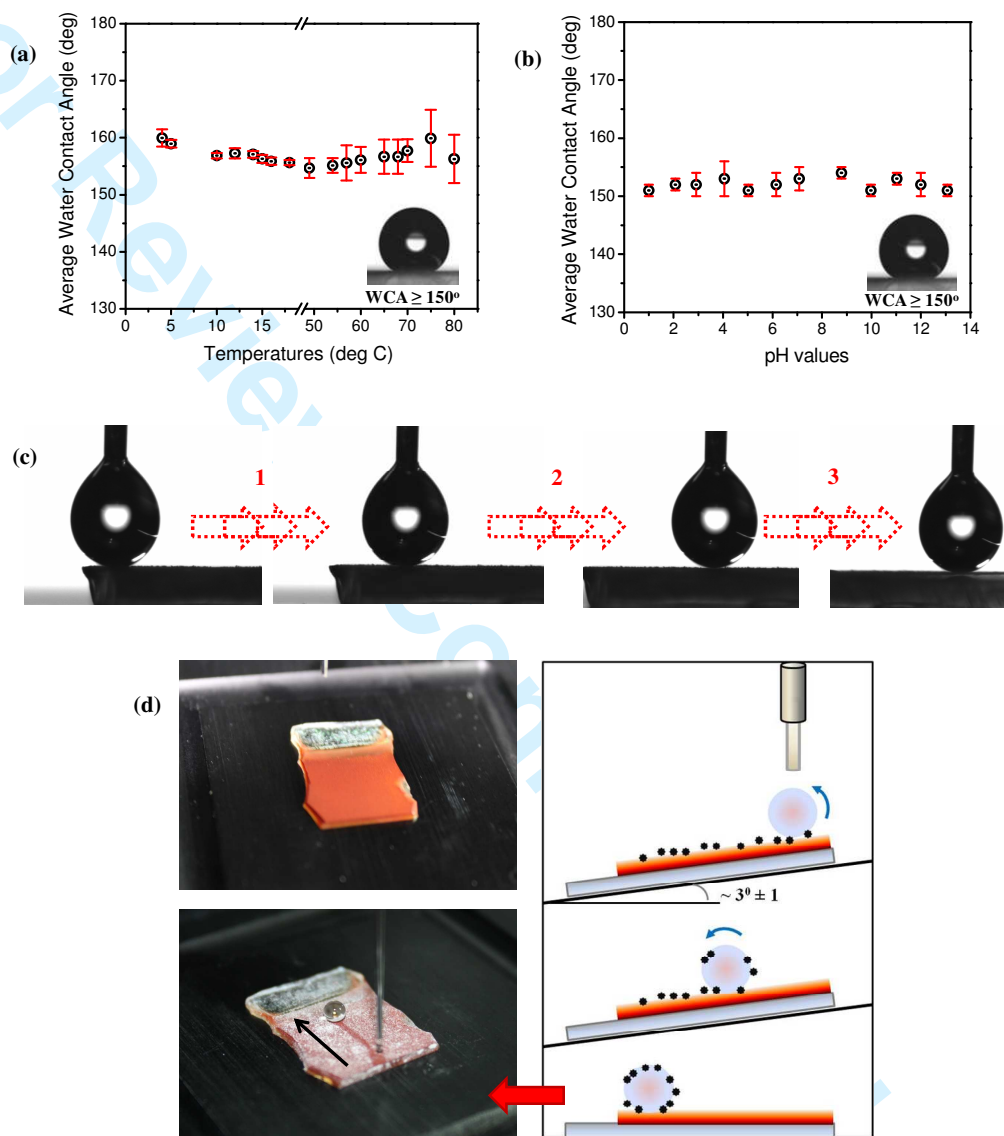

Figure 4. Static water contact angle measurements of the superhydrophobic polymeric surface at (a) low and high temperatures and at (b) different pH values of water. (c) Digital photo images of the actual movement of the water droplet along the superhydrophobic surface. (d) Digital photo images of the superhydrophobic surface before (top-left, pristine) and after (bottom-left, dusted surface) self-cleaning studies (right) at sliding angle of $3^\circ \pm 1$.

2.3 Switchable Surface Wettability

The redox property of the cross-linked conducting polymer film was investigated by applying a constant oxidation potential of 1.05 V using the same three electrode system in a monomer free condition. The applied voltage was determined from the peak potential of the CV diagram (Fig. 3a) in the anodic scan during the electropolymerization of the terthiophene monomer. Previously, our group has investigated the redox property of the conducting polymers of polycarbazole and polythiophene using *in-situ* measurements.[35] However, the surface wettability of the electrodeposited conducting polymers was not studied. In order to examine the change in the redox property of the polymer film, the electrodeposition of the conducting polymer was done in a transparent conducting substrate like ITO such that UV-Vis measurements can be performed. Prior to the application of the constant positive potential, the UV spectrum shows a maximum absorption peak (λ_{max}) at 440 nm, which is known as the π-π^* transision of the polythiophene film (upper curve of Fig. 5a).[36] At this condition of the film, the conducting polymer is considered to be neutral or undoped. Then after applying a potential of 1.05 V to the electrodeposited film, the spectrum displays a new broad peak between 600 to 800 nm (Fig. 5a bottom curve), which is due to the formation of polarons [37] of the conjugated polythiophene species and their complex redox ion couple with hexafluorophosphate ions (PF_6^-). During the application of the oxidation potential, the conducting polymer is known to become positively charged, and thus accepts the negatively charged counter ions (called dopants) from the supporting electrolyte in the bulk solution to maintain its neutrality and this process is referred as electrochemical doping.[38] As determined from the contact angle (inset of Figure 5a), the doping of the poly(G0-3T COOR) on PS coated substrate instigated the change in the wettability of the surface, which is attributed to the change in surface morphology and the effect of the dopant.[39] The change in surface morphology is evident in Figure 2c and 2d over wide scan areas. For instance, a rougher and highly porous surface is seen with the dedoped film (Fig. 2d and Fig. S3b-d), resulting to greater volume of trapped-air (Cassie-Baxter model[33]). At the same time, the surface of the dedoped film contains smaller hierarchical roughness of the submicron

range (Fig. S3b and S3d). Upon doping such as the application of 1.05 V, the polythiophene film may have possibly collapsed and the counter ions may have occupied the pores, and thus the surface is seen to be relatively less rough (Fig. 2c). Then upon dedoping the conducting polymer such as the application of 0 V, its morphology with a very rough and porous surface is restored (Fig. 2d). During the dedoping process, the polymer film is believed to eject the counter ion back into the bulk solution and returns to its neutral state,[38] which is proven by the appearance of the same UV spectrum with only one absorption peak maximum at 440 nm. The application of the oxidation potential of 1.05 V has easily converted the superhydrophobic surface (WCA $\geq$ 150°) into hydrophilic surface with WCA of $\sim$ 60°. Then upon dedoping the same surface, the polythiophene film is switched back to superhydrophobic state with a WCA equivalent to 152° $\pm$ 1. The reversibility of the surface wettability and color of the colloidally-templated polythiophene film *via* potential switching between 0 V and 1.05 V is shown in Figure S4. *Note that the reversible change in wetting (superhydrophobic to hydrophilic and back) with simultaneous change in color or electrochromism (orange to dark green and back) is also a unique aspect of these films.* Based from these results, the poly(G0-3T COOR)/PS surface can be considered as a stimuli responsive material.

The doping/dedoping of the polythiophene was further confirmed by XPS measurements. The high resolution XPS scans display the flourine (F1s) peak (Fig. 5b) between 682 - 688 eV and phosphorus (P 2p) peak (Fig. 5c) between 133 to 137 eV in the doped polymer surface, which are due to the PF_6^- (counter ion from the supporting electrolyte, TBAH). These peaks were not present upon dedoping of the same polymeric surface. The appearance of these unique elemental markers, which are due only to the counter ion, verifies the electrochemical doping of the electrodeposited conducting polymer. Interestingly, it is the absence of the fluorine peak (from TBAH dopant) that facilitates superhydrophobicity for this film. The sulfur peak (S 2p), which is the signature peak of the polythiophene, was also scanned in the XPS before and after doping to check for the stability of the conducting polymer. The presence of the S 2p peak (Fig. S5) at the same position and similar intensity

signifies that the conducting polymer is highly stable and is not impaired by the electrochemical doping

at the present condition.
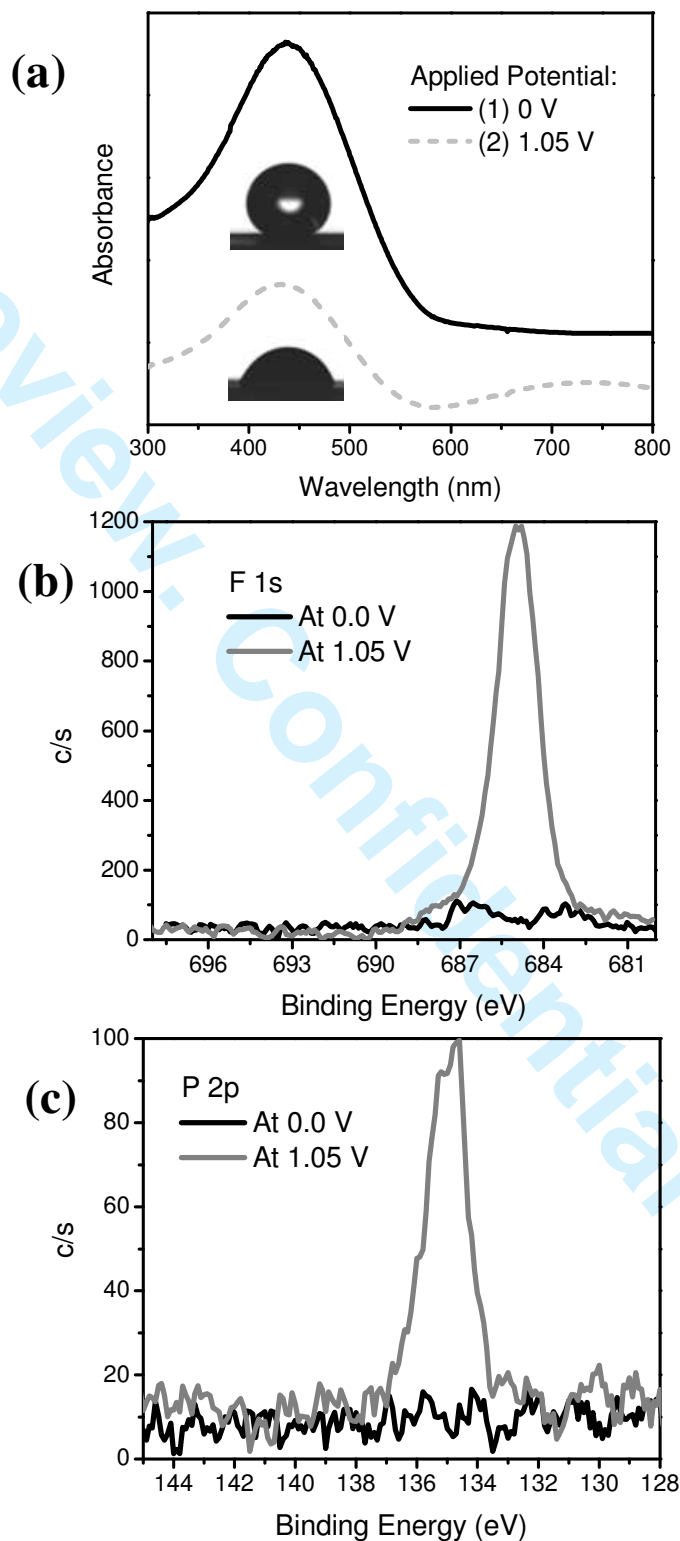
Figure 5. (a) UV-Vis spectrum and XPS high resolution peak of (b) fluorine and (c) phosphorus before
and after doping of the poly(G0-3T COOR) film.

2.4 Protein Adsorption Studies

The fabricated superhydrophobic surface was then tested for protein adsorption using fibrinogen protein as a model, which is a plasma protein present in relatively large quantities in the blood (0.2-0.4%), and plays a vital role in clot formation. This plasma protein has a size of 340 kDa and is commonly used to evaluate the biocompatibility or thrombogenesis of material surfaces, since it is known to absorb to most material surfaces.[40]

Table 1. Summary of the QCM measurements in air of fibrinogen adsorption on different surfaces.

Substrate	ΔF (Hz)	Ave. Mass Density* ($\mu g \cdot cm^2$)
1. Poly(G0-3T COOR)/PS Au, Undoped Film	-99.64	1.75
2. Poly(G0-3T COOR)/PS Au, Doped Film	-565.01	9.90
3. Bare Au	-308.29	5.40
4. Poly(G0-3T COOR)/PS Au, Undoped Film Injection of PBS solution only (control)	-101.10	1.77

*Calculated using the Sauerbrey equation (Equation 2 in Supporting Information).
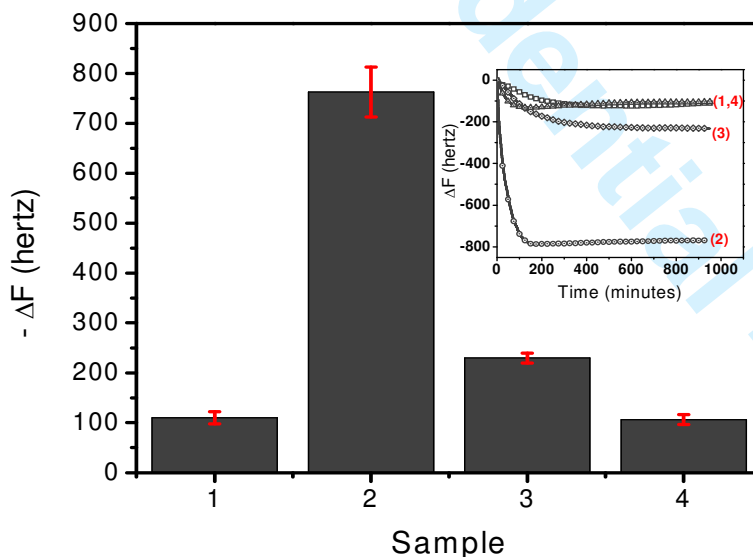

Figure 6. Bar graph summary with inset of the in-situ binding kinetic curve (average curve, n=3) of the QCM measurements of fibrinogen adsorption (1 mg/mL in PBS buffer, ~950 minutes) on different surfaces: (1) poly(G0-3T COOR)/PS Au undoped, (2) poly(G0-3T COOR)/PS Au doped (1.05 V, 30 mins), (3) bare Au, and (4) PBS injection to poly(G0-3TCOOR)/PS Au undoped (control film).

To determine the amount of protein adsorbed onto the electropolymerized colloidally-templated surface, quartz crystal microbalance (QCM) was used. The Sauerbrey equation (Supporting Information, Equation 2) was used to quantify the amount of fibrinogen adsorbed on different surfaces and the results are summarized in Table 1. The undoped poly(G0-3T COOR)/PS Au surface, which was determined to be superhydrophobic, had the least change in delta frequency (ΔF). Its measured value was similar to the ΔF when a PBS solution was injected into the same surface (control experiment). Furthermore, a positive control experiment was also done by simply injecting the same protein into the unmodified Au substrate. As expected, a higher change in ΔF was obtained, which is possibly due to the non-specific adsorption of protein. This finding implies that the undoped surface is highly resistant to the adsorption of fibrinogen. The change in the ΔF (~100 Hz) upon injection of the buffer to the undoped surface is attributed to the possible intake of PBS ions or water molecules into the surface. This is possible since the surface is highly porous as observed in the SEM (Fig. S3). Moreover, the N_2 drying after protein incubation may not be enough to completely dry the surface. However, upon doping the same surface, it allowed the adsorption of more protein with a significant decrease in the change in frequency (ΔF) by more than seven-fold. This result indicates that the same surface can be switched from inhibitory to adsorptive for proteins by simply doping/dedoping the polymeric surface, and thus potentially useful for making smart or tunable films that are stimuli responsive.

The QCM measurements in dry state was also validated by the analysis in solution (Fig. 6) that showed the same trend with the least and significant change in ΔF in the undoped superhydrophobic and in the doped surfaces, respectively. Also, the adsorption of fibrinogen onto the electrodeposited poly(G0-3T COOR) on bare Au was measured, and the binding curve is shown in Figure S6 that shows relatively protein adsorption resistancy of the surface as compared to the unmodified Au surface. The differences in the ΔF value between the QCM measurements in dry state and in solution can be credited to the effect of washing step (injection of milli-Q water to minimize/remove the salts) or N_2 drying after

incubation with the protein solution.

The results of the QCM measurements were further verified by contact angle, ATR IR, and XPS analyses. From the static contact angle, the undoped polymeric surface remains superhydrophobic (WCA ≥ 150°) even after incubation in the protein solution for ~950 minutes (Fig. 7a-top row), which means that the surface is highly repellent to fibrinogen over long periods of time. However, upon doping the same surface and incubating with a protein solution, the contact angle increased from 58° ± 1 to 96° ± 6 (Fig. 7a-bottom row), due to fibrinogen adsorption. The increased in contact angle is expected since the adsorbed fibrinogen will expose its hydrophobic domains in air.[41] The result of the contact angle was corroborated with the results of the ATR IR analysis (Fig. 7b). The undoped polymeric surface has shown similar IR spectrum even after dipping it in the protein solution. However, after doping the polymeric surface and immersing into a fibrinogen solution, the spectrum of the doped surface showed new peaks in the range of 3100 - 3600 cm^{-1}, attributed to the OH and NH stretching vibrations[42] from the protein.[41] Based on previous reports, the NH stretch correspond mostly to the lysine and arginine side groups of the αC domain of fibrinogen.[41] To further confirm that the protein is really adsorbed onto the doped polymeric surface, XPS analysis was also performed. The wide XPS scan (Fig. 7c) reveals a strong N 1s peak at 400 eV, which is an elemental marker for the fibrinogen proteins. This element is not present in the colloidally-templated electrodeposited polythiophene. A high resolution scan of the nitrogen element (inset of Fig. 7c) was also performed to verify the result. As expected, a prominent N 1s signal appears between 398 – 402 eV. Therefore, these results support that fibrinogen has adsorbed onto the doped polymeric surface.
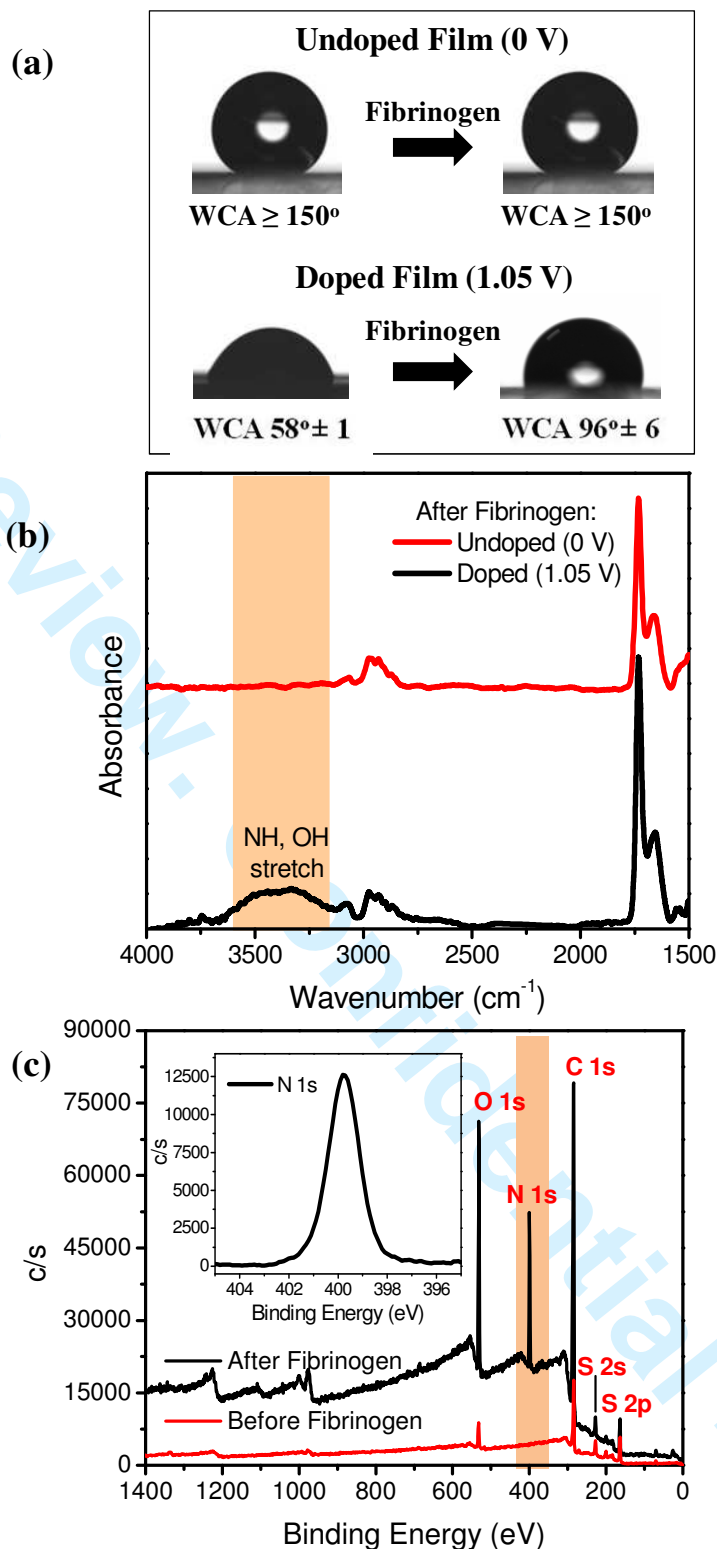
Figure 7. Static water contact angle and ATR IR measurements of the undoped and doped poly(G0-3T COOR)/PS Au surface after fibrinogen adsorption (1 mg/ml in PBS buffer, ~950 minutes). (c) XPS wide scan of the doped (1.05 V) poly(G0-3T COOR) before and after fibrinogen adsorption with inset of N 1s high resolution scan.

The resistance to protein adsorption onto the undoped polymeric surface can be explained by the fact that superhydrophobic surfaces prevent attachment of the biofouler dissolved in aqueous solution,[24] i.e. the contact between water and surface is minimized possibly due to the formation of the gas-liquid interface[32a, 33] with the muti-scale structuring.[10b] On the other hand, the adhesion of fibrinogen onto the doped polymeric surface can be ascribed to the increased contact between the aqueous media that contains the protein and the hydrophilic surface. Moreover, the adsorption of protein can also be related to the electrostatic interaction between the positively charged surface and the negatively charged protein. Note that fibrinogen has an isoelectric point of 5.5 and have a net negative charge in PBS buffer at pH 7.4.[43] Our results are consistent with the earlier findings of Chen and co-workers[1c] that their oxygen plasma treated Teflon superhydrophobic surface resisted the adsorption of protein similar to a PEG surface. However, upon switching the same surface into wettable state (more hydrophilic) by charging with an electric field, it promoted the adhesion of protein.

2.5 Bacteria Adhesion Studies

The ability of the surfaces to inhibit bacterial attachment was tested by incubating the films with the model bacteria *E. coli* for 2 h. Figure 8 presents the fluorescent images of the *E. coli* adsorbed onto the undoped and doped colloidally-templated polymeric surfaces after staining with SYTO 9 dye. A control experiment was also performed by incubating the bacterial solution in an unmodified ITO surface. Significant reduction of bacterial adhesion was observed for the undoped surface ($p < 0.05$) as compared to the control and the doped film. This outcome is consistent with the previous results of Liu et al.[44] that bacterial adhesion can be significantly reduced on a superhydrophobic surface.

Based on the results, the prevention of bacterial cell adhesion on the dedoped surface can be explained by the low binding strength between the bacteria and the surface because of the minimized contact between the aqueous media that suspends the bacteria and the surface.[24] Nonetheless, the adhesion of more bacteria onto the doped surface is possibly due to the hydrophilic nature of the surface that favors a better contact between the aqueous media and the surface. This result is confirmed when the

unmodified ITO, which is more hydrophilic and has a relatively smooth surface than the doped and

undoped surfaces, adhered the highest amount of bacteria (Fig. 8d). Moreover, we cannot discount that

the increased bacterial attachment can be related also to the electrostatic interaction between the net

positively-charged polymeric surface, created upon doping and the negatively charged *E. coli*.[45]

Although the determination of the exact mechanism of the bacterial adhesion is beyond the scope of this

publication, it is possible that the doped surface would have some antimicrobial properties, with

possible mechanisms similar to cationic peptides.[46]
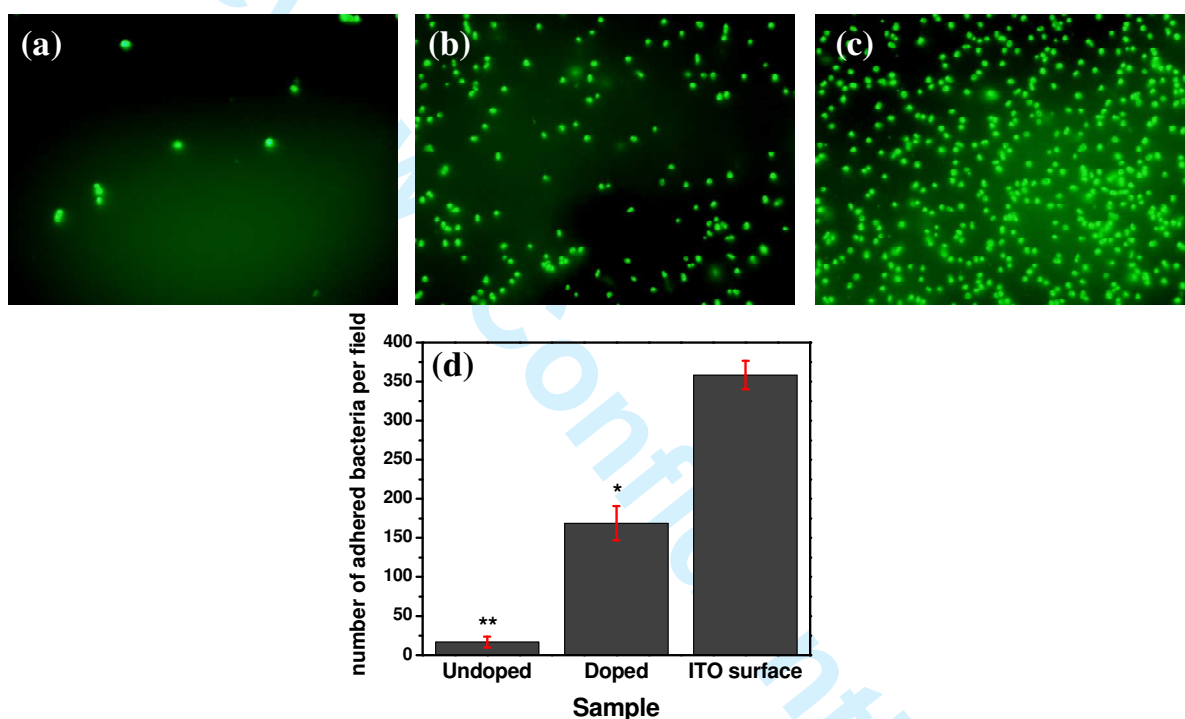
Figure 8. Bacterial adhesion during the 2 h incubation in *E. coli* solution and briefly washed by PBS buffer on the unit area of different surfaces ($1mm^2 \times 1mm^2$): (a) Undoped poly(G0-3T COOR)/PS Au, (b) doped (1.05 V) poly(G0-3T COOR)/PS Au, and (c) bare ITO (control). (d) Bar graph summary of the statistical analysis of the bacterial cell adhesion on the three surfaces. Notes: (1) values are averages with standard deviations of at least 8 pictures conducted on a minimum of two separate experiments. (2) * denotes significant difference in terms of the bacterial adhesion compared to the unmodified control ($p<0.05$, ANOVA on ranks). (3) ** denotes significant difference in terms of the bacterial adhesion compared to the doped ($p<0.05$, ANOVA on ranks)

3. CONCLUSIONS

Prevention of protein and bacterial adhesion was demonstrated on an anti-wetting and self-cleaning superhydrophobic polythiophene film fabricated using a combined particle-layering by LB-*like* method and CV-electropolymerization technique. The fabricated colloidally-templated polymeric surface has proven to be highly stable and non-wetting over a wide pH range (pH 1-13), temperatures (between 4 ^{o}C and 80 ^{o}C) and even when the surface was frozen at -10 ^{o}C for more than 4 days. Furthermore, the superhydrophobic surface has demonstrated self-cleaning at a sliding angle of about 3°. By simply manipulating the redox property of the conducting polymer using an external stimuli (e.g. applying a constant potential), the wettability of the surface was easily changed, which affected the adhesion of fibrinogen and *E. coli.* Since the switching of the surface wettability can be easily achieved by simply changing the redox property of the conducting polymer, the proposed methodology maybe useful for fabricating smart coatings onto various conducting surfaces, which can be tuned to resist or adsorb protein and bacterial cell. Current effort is underway for testing the superhydrophobic surface on other proteins and bacterial cells and towards understanding the various mechanism of their adhesion and resistance.

4. EXPERIMENTAL SECTION

Materials and Reagents. Polystyrene (PS) latex microbeads (0.5 μm in diameter, 2.5 wt % solids in aqueous suspension) were purchased from Polysciences, Inc. and were used without further purification. Acetonitrile (ACN), sodium *n*-dodecyl sulfate (SDS), and tetrabutylammonium hexafluorophosphate (TBAH), fibrinogen protein, phosphate buffer saline (PBS) tablet were obtained from Sigma-Aldrich. The glass slides (BK 7) for gold (Au) depositions were acquired from VWR. The tin-doped indium oxide, ITO ($In_2[Sn_x]O_{3-y}$, one side coated on glass, sheet resistance ≤ 30 Ωcm^{-2}) used for the preparation of superhydrophobic surface was purchased from SPI Supplies/Structure Probe, Inc. Prior to use, the ITO substrate was sonicated in Alconox detergent followed by rinsing with ultra pure water. The ITO

was then sonicated for 10 min in isopropanol, hexane, and then toluene, respectively, prior to oxygen

plasma cleaning for ~120 sec. The Au substrate also used for the fabrication of superhydrophobic

surface was prepared by thermally evaporating gold of 99.99% purity (50 to 100 nm thick) under high

vacuum (10^{-6} bar) onto the BK 7 glass slide with chromium adhesion layer (~10 nm thick). The Cr and

Au depositions were done at a rate of ~0.4 Å sec^{-1} and ~1.1 Å sec^{-1}, respectively, using a thermal

evaporator (Edwards). Prior to use, the Au-coated slide was also cleaned in the oxygen plasma cleaner

for ~120 sec. The deionized water or ultra pure water (resistivity ~18.2 MΩ.cm) used for the dilution of

PS particles was purified by a Milli-Q Academic® system (Millipore Cooperation) with a 0.22 micron

Millistack filter at the outlet. Fibrinogen solution was prepared in PBS solution at 1 mg/ml

concentration. The PBS buffer solution (0.1 M concentration, pH 7.4) was prepared by dissolving 1

tablet of the PBS into 200 ml of Milli-Q water. The monomer used in the electrochemical

polymerization was synthesized in our laboratory. And the details of the synthesis (Scheme S1) of ethyl

2-(2,5-di(thiophen-2-yl)thiophen-3-yl)acetate (abbreviated as G0-3T COOR where R=CH_2CH_3) are

reported in the supporting document.

Preparation of Superhydrophobic Surface. The superhydrophobic conducting surface was fabricated

by simple two-step process such as (1) layering of PS latex microbeads onto conducting substrates like

Au and ITO slides, and (2) electropolymerization of the monomer into the PS-coated slides. The

layering of PS latex beads was prepared using a similar procedure described earlier by Grady and co-

workers.[27] The substrate was attached vertically into the dipper motor *via* a Teflon clip and was dipped

into a solution of PS particles (1 wt % in Milli-Q water) and SDS (34.7 mM) as spreading agent. The

substrate was then withdrawn vertically from the solution at a lift-up rate of 0.1-0.3 mm/s. The substrate

was then dried by suspending it in air for a few min. After the layering of the latex spheres, the

monomer (5 mM G0-3T COOR in ACN with 0.1 M TBAH as supporting electrolyte) was

electropolymerized onto the PS-coated substrate (Au or ITO) as the working electrode in a standard

three electrode measuring cell with platinum (Pt) wire as the counter electrode and Ag/AgCl wire as the reference electrode. The electropolymerization was done using cyclic voltammetric technique in a fabricated electrochemical cell (Teflon made). The potential was scanned between 0 V to 1.1 V (and also 0V to 1.5 V) for 15 cycles at a scan rate of 5 mV/s. Note that the use of very low scan rate will result to the formation of thicker polymer coatings. Also, it is possible to do this deposition of polymer film by chronoamperometric or potentiostatic methods. After electrodeposition, the film was thoroughly washed in ACN (at least 3 times) to remove the excess monomer and physically adsorbed polymer or oligomer, and a post-polymerization monomer-free scan (in a solution of ACN with 0.1 M TBAH) was performed by using exactly the same electrochemistry set-up and settings but for 1 CV cycle only. Finally, the electropolymerized film was thoroughly dried in vacuum for at least 1 hr prior to any characterizations. To dope (or undoped) the polymeric surface, a constant oxidation potential of 1.05 V (or 0 V) was applied for 30 minutes onto the polymeric surface (working electrode), which was immersed in ACN with 0.1 M TBAH along with the reference (Ag/AgCl) and counter (Pt wire) electrodes.

Characterizations. Cyclic voltammetry (CV) was performed in a fabricated electrochemical cell (Teflon-made, with a diameter of 1.0 cm and volume of 0.785 cm^3) using a conventional three-electrode cell using an Autolab PGSTAT 12 potentiostat (Brinkmann Instruments now Metrohm USA, Inc.). The potentiostat is controlled by GPES software (version 4.9).

Profilometry of model Alpha-Step 200 was used to measure the thickness of the polymeric surface. The Alpha-Step 200 profilometer can accurately measure the surface profiles below 200 Å and up to 200 µm. A low stylus force of 5 mg was used during the scanning to avoid damaging the polymer surface. The measurements were done at least 10 times on different areas of the sample surface under ambient and dry conditions.

The static contact angle measurements were done using a CAM 200 optical contact angle meter (KSV

Instruments Ltd) with CAM 200 software. The experiment was carried out by slowly moving upward

the sample stage with the sample surface on top to come close onto the water droplet (~1 µL) that was

suspended at the tip of the micro syringe (200 µL). The reading of the contact angle was done after 30

seconds when the droplet has been made into the surface. The measurements were performed for at least

five trials at different areas of the sample surface and were replicated in three more samples. *Note that*

the WCA value was acquired only when the water droplet was dropped at a relatively far distance (ca

0.3 cm) away from the surface since no reading can be measured if the droplet is to come into contact

with the substrate. For dynamic contact angle measurements, the angles were measured using a Ramé-

Hart model 100 contact angle goniometer. The liquids were dispensed and withdrawn using a Matrix

Technologies micro-Electrapette 25. Contact angles were collected and averaged from measurements on

four distinct slides using three separate drops per slide.

Atomic force microscopy (AFM) analysis was carried out in a piezo scanner from Agilent

Technologies. The scanning rate was between 0.8-1.5 lines/s. Commercially available tapping mode

tips (TAP300, Silicon AFM Probes, Ted Pella, Inc.) were used on cantilevers with a resonance

frequency in the range of 290-410 kHz. The scanning of the PS-coated Au and ITO was performed

under ambient and dry conditions. All AFM topographic images (AAC tapping mode) were filtered and

analyzed by using Gwyddion software (version 2.19). Only the PS-coated substrates were scanned in the

AFM. Because of the formation of very rough surfaces, the electropolymerized films on PS-coated

substrates were only scanned in the SEM.

The attenuated total reflection infrared (ATR FTIR) spectra were obtained on a Digilab FTS 7000

equipped with a HgCdTe detector from 4000 to 600 (cm^{-1}) wavenumbers. All spectra were taken with a

nominal spectral resolution of 4 cm^{-1} in absorbance mode. All films were measured under ambient and

dry conditions for several trials at different areas of the sample surface.

The morphology of the samples was examined by field emission scanning electron microscopy (FE-

SEM) using a JSM 6330F JEOL instrument operating at 15 kV. Prior to SEM analysis, the films were

thoroughly dried under vacuum for at least 24 hrs.

Quartz crystal microbalance (QCM) measurement was used for the adsorption of fibrinogen. The QCM apparatus, probe, and crystals were made available from Maxtek Inc. (Inficon). The AT-cut polished QCM crystals (5 MHz) was used as the working electrode. The data acquisition was done with an R-QCM system equipped with a built-in phase lock oscillator and the R-QCM Data-Log software. The QCM crystals were also cleaned (~120 sec) with an oxygen plasma etcher (Plasmod, March) immediately prior to use. The measurement was done by allowing a stable baseline in air prior to the injection of the protein solution. The QCM crystal with the polymeric surface was incubated in the fibrinogen solution (1 ml volume) for ~950 minutes. Afterwards, the protein solution was removed using micro pipette, and the crystal was rinsed with Milli-Q water to eliminate/minimize the salts from the PBS buffer. Then a stable baseline in air was again achieved after drying in the N_2 gas.

BACTERIAL ADHESION MEASUREMENTS.

Bacterial Culture: A single isolated *Escherichia coli* K12 MG1655 (*E. coli*) colony was inoculated in 5 mL Tryptic Soy Broth (TSB) overnight at 35 ^{o}C. The bacterial culture was centrifuged at 3000 rpm for 10 minutes, and the bacteria pellet was resuspended in TSB. The optical density of the suspension was adjusted to 0.5 at 600 nm, which corresponds to a concentration of 10^7 colony forming units per milliliters (CFU/ml). The doped, undoped colloidal-polymeric films and unmodified ITO substrate were individually placed in a 12 well-plate (Falcon). To each well was added 1.0 ml of bacterial culture and then incubated at 37 °C (without shaking) for 2 h. The samples were then removed and immediately prior to viewing were stained with 3μl of SYTO 9 dye solution for 10 minutes from Molecular Probes (Leiden, The Netherlands) marking viable bacterial cells. The surfaces were placed in microscope slides, covered with a cover slip and imaged using BX 51 Olympus Fluorescent Microscope equipped with a DP72 digital camera under 100*x* objective. All images were acquired and analyzed using cell Sens Dimension software (Olympus).

Statistical analysis. The amount of attached bacterial cells was expressed as the mean number of bacteria ± standard deviation of four experiments (3 replicates prepared at 2 different times). Statistical differences between median values were done using pair-wise comparison by ANOVA on ranks test using Sigma Plot Software (version 11). Significance was accepted at a level of $p < 0.05$.

ASSOCIATED CONTENT

Supporting Information. Details of the synthesis and NMR spectrum of the monomer (ethyl 2-(2,5-di(thiophen-2-yl)thiophen-3-yl)acetate or G0-3T COOR), AFM images of the different sizes of PS, SEM images superhydrophobic polythiophene films, static water contact angle of the undoped and doped polythiophene films, XPS S2p spectrum of the polythiophene film, QCM kinetic plot of fibrinogen adsorption on different surfaces, and Sauerbrey equation. This material is available free of charge via the Internet at http://pubs.acs.org/.

AUTHOR INFORMATION

Corresponding Author

* E-mail: radvincula@uh.edu; Phone: +1 713 743 1755.

Present Address

Department of Chemistry and Department of Chemical and Biomolecular Engineering, University of Houston, Houston, Texas 77204-5003.

REFERENCES

(1) (a) Feng, X. J.; Jiang, L. *Adv. Mater.* **2006,** *18,* 3063. (b) Blossey, R. *Nature Mater.* **2003,** *2,* 301. (c) Shiu, J-Y.; Chen, P. *Adv. Funct. Mater.* **2007,** *17,* 2680.

(2) Barthlott, W.; Neinhuis, C. *Planta* **1997**, *202*, 1.

(3) (a) Mock, U.; Förster, R.; Menz, W.; Rühe, J. *J. Phys. Condens. Matter* **2005**, *17*, S639. (b) Otten, A.; Herminghaus, S. *Langmuir* **2004**, *20*, 2405.

(4) (a) Gao, X. F.; Jiang, L. *Nature* **2004**, *432*, 36. (b) Wagner, T.; Neinhuis, C.; Barthlott, W. *Acta Zool.* **1996**, *77*, 213. (c) Lee, W.; Jin, M. K.; Yoo, W. C.; Lee, J. K. *Langmuir* **2004**, *20*, 7665.

(5) Ma, M.; Hill, M. *Curr. Opin. Colloid In.* **2006,** *11,* 193.

(6) Darmanin, T.; Guittard, F. *J. Am. Chem. Soc.* **2009,** *131,* 7928.

(7) (a) Houde, M. ; Martin, J. W. ; Letcher, R. J. ; Solomon, K. R. ; Muir, D. C. G. *Environ. Sci. Technol.* **2006,** *40,* 3463. (b) Giesy, J. P. ; Kannan, K. *Environ. Sci. Technol.* **2001,** *35,* 1339.

(8) (a) Huang, J-H.; Yang, C-Y.; Hsu, C-Y.; Chen, C-L.; Lin, L-Y.; Wang, R-R.; Ho, K-C.; Chu. C-W. *ACS Appl. Mater. Interfaces* **2009,** *1,* 2821. (b) Welsh, D. M.; Kloeppner, K. J.; Madrigal, L.; Pinto, M. R.; Schanze, K. S.; Abboud, K. A.; Powell, D.; Reynolds, J. R. *Macromolecules* **2002**, *35*, 6517. (c) Schwendeman, I.; Hwang, J.; Welsh, D. M.; Tanner, D. B.; Reynolds, J. R. *Adv. Mater.* **2001**, *13*, 634. (d) Gaupp, C. L.; Welsh, D. M.; Reynolds, J. R. *Macromol. Rapid Commun.* **2002**, *23*, 885. (d) Kumar, A.; Welsh, D. M.; Morvant, M. C.; Abboud, K.; Reynolds, J. R. *Chem. Mater.* **1998**, *10*, 896. (e) Kumar, A.; Reynolds, J. R. *Macromolecules* **1996**, *29*, 7629.

(9) Genzer, J.; Efimenko, K. *Biofouling* **2006,** *22,* 339.

(10) (a) Shiu, J-Y.; Kuo, C-W.; Whang, W-T.; Chen, P. *Lab Chip,* **2010,** *10,* 556. (b) Koc, Y.; de Mello, A. J.; McHale, G.; Newton, M. I.; Roach, P.; Shirtcliffe, N. J. *Lab Chip,* **2008,** *8,* 582.

(11) Benmakroha, Y.; Zhang, S.; Rolfe, P. *Med. Bio. Eng. Comput.***1995**, *33*, 811.

(12) Kumar, N.; Parajuli, O.; Hahm, J-I. *J. Phys. Chem. B* **2007,** *111,* 4581. (b) Kumar, N.; Hahm, J.-I.; *Langmuir* **2005,** *21,* 6652. (c) Liu, D.; Wang, T.; Keddie, J. L. *Langmuir* **2009,** *25,* 4526.

(13) (a) Park, J. Y.; Yoo, Y. J. *Appl. Microbiol. Biotechnol.* **2009,** *82,* 415. (b) Dash; R. R.; Gaur, A.; Balomajumder, C. *J. Hazard. Mater.* **2009,** *163,* 1.

(14) (a) Yakimov, M. M.; Timmis, K. N.; Golyshin, P. N. *Curr. Opin. Biotechnol.* **2007,** *18,* 257. (b) Gavrilescu, M.; Pavel, L. V.; Cretescu, I. *J. Hazard. Mater.* **2009,** *163,* 475. (c) Vinther, F. P.; Brinch, U. C.; Elsgaard, L.; Fredslund, L.; Iversen, B. V.; Torp, S.; Jacobsen, C. S. *J. Environ. Qual.* **2008,** *37,* 1710. (d) Castillo Mdel, P.; Torstensson, L.; Stenstrom, J. *J. Agric. Food Chem.* **2008,** *56,* 6206.

(15) (a) Close, M.; Dann, R.; Ball, A.; Pirie, R.; Savill, M.; Smith, Z. *J. Water Health* **2008,** *6,* 83. (b) Dopson, M.; Halinen, A. K.; Rahunen, N.; Bostrom, D.; Sundkvist, J. E.; Riekkola-Vanhanen, M.; Kaksonen, A. H.; Puhakka, J. A. *Biotechnol. Bioeng.* **2008,** *99*, 811.

(16) Shen, M.; Wagner, M. S.; Castner, D. G.; Ratner, B. D.; Horbett, T. A. *Langmuir* **2003,** *19,* 1692.

(17) (a) Mrksich, M.; Sigal, G. B.; Whitesides, G. M. *Langmuir* **1995,** *11,* 4383. (b) Goodman, S. L.; Simmons, S. R.; Cooper, S. L.; Albrecht, R. M. *J. Colloid Interface Sci.* **1990,** *139,* 561.

(18) (a) Sigal, G. B.; Mrksich, M.; Whitesides, G. M. *J. Am. Chem. Soc.* **1998,** *120,* 3464. (b) Baier, R. E. ; Meyer, A. E.; Natiella, J. R.; Natiella, R. R. ; Carter, J. M. *J. Biomed. Mater. Res.* **1984,** *18,* 337.

(19) Frentzen, M.; Oxborn, J. F.; Nolden, R. *Dtsch. Zahnaerzd Z.* **1988,** *43,* 719.

(20) Tsvetanova, Z. *Chemicals as Intentional and Accidental Global Environmental Threats;* Springer: Netherlands, **2006,** 463.

(21) (a) Chapman, R. G.; Ostuni, E.; Liang, M. N.; Meluleni, G.; Kim, E.; Yan, L.; Pier, G.; Warren, H. S.; Whitesides, G. M. *Langmuir* **2001,** *17,* 1225. (b) Sadana, A. *Chem. Rev.* **1992,** *92,* 1799.

(22) (a) Banerjee, I.; Pangule, R. C.; Kane, R. S. *Adv. Mater.* **2011,** *23,* 690. (b) Pompe, T.; Zschoche, S.; Herold, N.; Salchert, K.; Gouzy, M-F.; Sperling, C.; Werner, C. *Biomacromolecules*, **2003**, *4,* 1072. (c) Johnell, M.; Larsson, R.; Siegbahn, A. *Biomaterials* **2005**, *26*, 1731. (d) Klement, P.; Du, Y. J.; Berry, L.; Andrew, M.; Chan, A. K. C. *Biomaterials* **2002**, *23*, 527. (e) Ferrer, M. C. C.; Yang, S.; Eckmann, D. M.; Composto, R. J. *Langmuir* **2010,** *26,* 14126. (f) Liu, M.; Yue, X.; Dai, Z.; Ma, Y.; Xing, L.; Zha, Z.; Liu, S.; Li, Y. *ACS Appl. Mater. Interfaces*, **2009**, *1* 113. (g) Rabinow, B. E.; Ding, Y. S.; Qin, C.; Mchalsky, M. L.; Schneider, J. H.; Ashline, K. A.; Shelbourn, T. L.; Albrecht, R. M. *J. Biomater. Sci. Polym. Ed.* **1994**, *6*, 91. (h) Lehmann, T.; Ruhe, J. *Macromol. Symp.* **1999**, *142*, 1. (i) Benhabbour, S. R.; Liu, L.; Sheardown, H.; Adronov, A. *Macromolecules*, **2008**, *41*, 2567. (k) Prime, K. L.; Whiteside, G. M. *J. Am. Chem. Soc.* **1993**, *115*, 10714. (c) Gombotz, W. R.; Guanghui, W.; Horbett, T. A.; Hoffman, A. S. *J. Biomed. Mater. Res.* **1991**, *25*, 1547. (l) Jeon, S. I.; Andrade, J. D.; de Gennes, P. G. *J. Colloid Interface Sci.* **1991**, *142*, 159. (m) Grunze, M.; Harder, P.; Spencer, N. D.; Hahner, G.; Feldman, K. *J. Am. Chem. Soc.* **1999**, *121*, 10134. (n) Prime, K. L.; Whitesides, G. M. *Science* **1991**, *252*, 1164. (o) Reisch, A.; Voegel, J-C.; Gonthier, E.; Decher, G.; Senger, B.; Schaaf, P.; Mésini, P. J. *Langmuir* **2009,** *25,* 3610. (p) Reisch, A.; Hemmerlé, J.; Voegel, J-C.; Gonthier, E.; Decher, G.; Benkirane-Jessel, N.; Chassepot, A.; Mertz, D.; Lavalle, P.; Mésini, P.; Schaaf, P. *J. Mater. Chem.* **2008,** *18,* 4242.

(23) (a) Bers, A. V.; Wahl, M. *Biofouling* **2004,** *20,* 43. (b) Hoipkemeier-Wilson, L.; Schumacher, J. F.; Carmen, M. L.; Gibson, A. L.; Feinberg, A. W.; Callow, M. E.; Finlay, J. A.; Callow, J. A.; Brenan, A. B. *Biofouling* **2004,** *20,* 53. (c) Zhang, H.; Lamb, R.; Lewis, J. *Sci. Technol. Adv. Mater.* **2006,** *6,* 236.

(24) Marmur, A. *Biofouling* **2006,** *22,* 107.

(25) Lichter, J. A.; Van Vliet, K. J.; Rubner, M. F. *Macromolecules* **2009,** *42,* 8573.

(26) (a) Pernites, R. B.; Ponnapati, R. R.; Advincula, R. C. *Macromolecules* **2010,** *43,* 9724. (b) Pernites, R. B.; Ponnapati, R. R.; Felipe, M. J.; Advincula, R. C. *Biosens. Bioelectron.* **2011,** *26,* 2766.

(27) Marquez, M.; Grady, B. P. *Langmuir* **2004,** *20,* 10998.

(28) Lange, U.; Roznyatouskaya, N. V.; Mirsky, V. M. *Anal. Chim. Acta* **2008,** *614,* 1.

(29) Apodaca, D. C.; Pernites, R. B.; Ponnapati, R. R.; Del Mundo, F.; Advincula, R. C. *ACS Appl. Mater. Interfaces* **2011,** *3,*191.

(30) (a) Rasch, B.; Vielstich, W. *J. Electroanal. Chem.* **1994,** *370,* 109. (b) Roncali, J. *Chem. Rev.* **1992,** *92,* 711-738.

(31) Miwa, M.; Nakajima, A.; Fujishima, A.; Hashimoto, K.; Watanabe, T. *Langmuir* **2000,** *16,* 5754.

(32) (a) Steele, A.; Bayer, I.; Loth, E. *Nano Lett.* **2009,** *9,* 501. (b) Johnson Jr., R. E.; Dettre, R. H. *Adv. Chem. Ser.* **1963,** *43,* 112.

(33) Cassie, A. B. D.; Baxter, S. *Trans. Faraday Soc.* **1944,** *40,* 546.

(34) Marmur, A. *Langmuir* **2003,** *19,* 8343.

(35) Taranekar, P.; Fulghum, T.; Baba, A.; Patton, D.; Advincula, R. C. *Langmuir* **2007,** *23,* 908.

(36) Xia, C.; Park, M-K.; Advincula, R. C. *Langmuir* **2001,** *17,* 7893.

(37) Ikeda, T.; Higuchi, M.; Kurth, D. G. *J. Am. Chem. Soc.* **2009,** *131,* 9158.

(38) (a) Deore, B.; Chen, Z.; Nagaoka, T. *Anal. Sci.* **1999,** *15,* 827. (b) Bredas, J. L.; Street, G. B. *Acc. Chem. Res.* **1985,** *18,* 309.

(39) Azioune, A.; Chehimi, M. M.; Miksa, B.; Basinska, T.; Slomkowski, S. *Langmuir* **2002,** *18,* 1150.

(40) (a) Ostuni, E.; Chapman, R. G.; Holmlin, R. E.; Takayama, S.; Whitesides, G. M. *Langmuir*, **2001**, *17,* 5605. (b) Chapman, R. G.; Ostuni, E.; Takayama, S.; Holmlin, R. E.; Yan, L.; Whitesides, G.

M. *J. Am. Chem. Soc*. **2000**, *122,* 8303. (c) Ostuni, E.; Chapman, R. G.; Liang, M. N.; Meluleni, G.; Pier, G.; Ingber, D. E.; Whitesides, G. M. *Langmuir*. **2001**, *17,* 6336.

(41) Clarke, M. L.; Wang, J.; Chen, Z. *J. Phys. Chem. B* **2005,** *109,* 22027.

(42) Yang, Q.; Strathmann, M.; Rumpf, A.; Schaule, G.; Ulbricht, M. *ACS. Appl. Mater. Interfaces* **2010,** *2,* 3555.

(43) Wei, T.; Kaewtathip, S.; Shing, K. *J. Phys. Chem. C* **2009,** *113,* 2053.

(44) Liu, T.; Dong, L.; Liu, T.; Yin, Y. *Electrochim. Acta* **2010**, *55,* 5281.

(45) (a) Bayer, M. E.; Sloyer Jr., J. L. *J. Gen. Microbio* **1990,** 136, 867. (b) Ghuysen, J. M.; Hackenbeck, R. *Bacterial Cell Wall*; Elsevier: Amsterdam, The Netherlands, **1994**.

(46) (a) Oren, Z.; Shai, Y. *Biopolymers* **1998**, *47*, 451. (b) Shai Y. *Biopolymers* **2002,** *66,* 236.